

Refractories Applications *Transactions*

Volume 4, Number 3

November/December 2009

Editorial Board

Jeffrey D. Smith, Editor, Missouri S&T, USA
Mary Lee, Assistant to the Editor, Missouri S&T, USA

Technical Referees

Esteban Aglietti, CETMC, Argentina
Richard C. Bradt, The University of Alabama, USA
Carmen Baudín, Instituto de Cerámica y Vidrio, Spain
Elena Brandaleze, Universidad Tecnológica Nacional, San Nicolás,
Argentina
Angel Caballero, Instituto de Cerámica y Vidrio, Madrid, Spain
William G. Fahrenholtz, Missouri S&T, USA
Geraldo E. Gonçalves, Magnesita S.A., Brazil
James G. Hemrick, Oak Ridge National Laboratory, USA
Orville Hunter, Consultant, USA
William E. Lee, University of Sheffield, UK
Li Nan, Wuhan University of Sci. & Tech., China
George Oprea, The University of British Columbia, Canada
Victor C. Pandolfelli, Universidade Federal de São Carlos, Brazil
Christopher Parr, Kerneos, France
Jacques Poirier, Polytech, Orleans, France
Michel Rigaud, École Polytechnique, Canada
Charles Semler, Semler Materials Services, USA
Mark Stett, Consultant, USA
Raul Topolevsky, Siderar, Argentina

All submissions should be sent to:

Mary Lee, Assistant to the Editor
Refractories Applications Transactions
Missouri S&T
Materials Science and Engineering Dept.
223 McNutt Hall
1870 Miner Circle Drive
Rolla, MO 65409-0330

Phone: (573) 341-6561
Fax: (573) 341-6934
E-mail: leem@mst.edu

For author guidelines please see those listed on the
Journal of the American Ceramic Society website:
<http://www.ceramics.org/publications/journal/authorinstructions.asp>

File Formats

Text: Microsoft Word.

Graphics: JPEG, TIFF or EPS created from supported
applications, PowerPoint, Acrobat PDF (PDF format is
acceptable for review purposes only)

Microsoft Word with embedded graphics.

Compression Software: WinZip (PC) or Stuffit
(Macintosh)

Resolution of graphics files must be at least 300 dpi for
halftones, 600 dpi for lettering, and 1200 dpi for line art.

Manuscript Number 040209

Refractories Applications *Transactions*

Effect of Celsian on Corrosion of Aluminosilicate Castable Refractories

Devdutt Shukla, Jeffrey D. Smith

Department of Materials Science and Engineering

Missouri University of Science and Technology, Rolla, MO 65409

(jsmith@mst.edu)

ABSTRACT

In-situ formation of BaAl₂Si₂O₈ (Ba-celsian) and SrAl₂Si₂O₈ (Sr-celsian) and the corresponding effect on corrosion resistance of aluminosilicate castable refractories was studied using static cup tests with molten AL 5083 alloy. Barium carbonate (BaCO₃) and strontium carbonate (SrCO₃) were added to an aluminosilicate castable refractory to form a celsian rich refractory matrix. Penetration and apparent porosity were measured for all tested compositions. Incremental additions of BaCO₃ and SrCO₃ successfully decreased aluminum penetration. Heating to 1300°C reduced corrosion by 25% compared to samples heated to 1200°C. Apparent porosity was also 50% lower compared to the same compositions heated to 1200°C. Corrosion was analyzed using x-ray diffraction and microscopic analysis. A Ba-celsian-rich, eutectic melt phase combined with Ba-celsian crystals providing a protective effect in samples heated to 1300°C. SrCO₃ also promoted the formation of mullite upon heating to 1200°C. Heating to 1300°C did not lead to significant reductions in apparent porosity. The current work suggests that corrosion resistance of aluminosilicate refractories may be improved by blocking the refractory pore network with a corrosion resistant, celsian rich phase formed under operating conditions.

INTRODUCTION

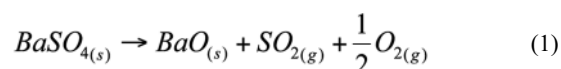
Aluminosilicate refractories are widely used as materials for linings in aluminum holding furnaces. Refractories for molten aluminum contact applications face severe corrosion and degradation issues due to the extremely reducing nature of molten aluminum alloy. Corrosion occurs in the form of a dense, grey, alumina-rich layer resulting from the reaction of refractory oxides such as silica with molten aluminum. Corundum formation is detrimental to the mechanical integrity of the refractory lining and to the thermal efficiency of the furnace¹⁻⁵. The focus of refractory development has shifted to minimizing aluminum attack using non-wetting additives such as BaSO₄, AlF₃, CaF₂ and AlTiO₃. A better understanding of the protection mechanism associated with these additives is desired^{1,2}.

Barium sulfate (BaSO₄) additions were made to aluminosilicate refractories to decrease wetting of the refractory and thereby reduce molten aluminum penetration into the refractory lining³. The patent stated that the additive would be effective up to 1700°F (927°C). Below this temperature, enhanced penetration resistance of conventional castable refractories has indeed been reported^{4,5}. In an effort to increase furnace productivity, however, operating conditions are often compromised. Furnace temperatures along sidewalls in the bellyband zone can reach as high as 1300°C⁵. These conditions result in penetration of refractories and corundum growth on previously successful castable compositions. The protective effect of BaSO₄ is apparently lost at high service temperatures.

Although the benefits of the addition of BaSO₄ have been successfully demonstrated in experimental studies, no comprehensive explanation of the protective mechanism provided by its addition was originally available. Recently, however, research efforts have focused on understanding

the mechanism of the benefits provided by BaSO₄. Studies have suggested that when refractories are heated to between 900 and 1200°C, BaSO₄ reacts with alumina and silica within the refractory to form barium aluminosilicate, commonly known as barium celsian (Ba-celsian)⁶. Formation of such a celsian phase reduced the amount of free silica within the matrix and consequently improved the corrosion resistance of the refractory^{7,8}. The effect of adding 7 wt% BaSO₄ to a high alumina refractory was studied by Gupta and Koshy, who also observed that the formation of celsian could dilute the corrosive influence of silica by reducing the proportion of free silica in the refractory⁹.

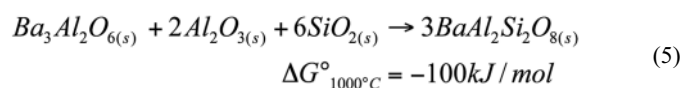
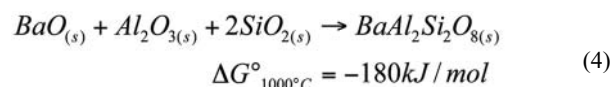
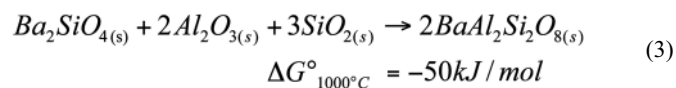
Afshar and Allaire have shown that BaSO₄ is completely consumed upon heating above 1000°C. Thermal-gravimetric analysis of BaSO₄ revealed that it decomposed at temperatures above 1150°C as described by the reaction^{1,3}:



Thus, above 1150°C, the role of BaSO₄ as an additive is limited to providing a source of BaO that can further react with oxides already present in the refractory to form barium aluminate and/or barium celsian based on the refractory composition. BaO reacts with silica to form barium orthosilicate by the reaction⁶:



This ortho-silicate reacts further with free silica and alumina within the matrix forming Ba-celsian by one or more reactions of the following type:



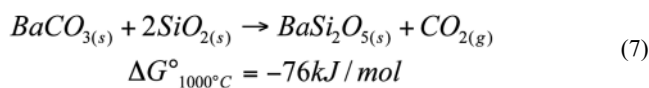
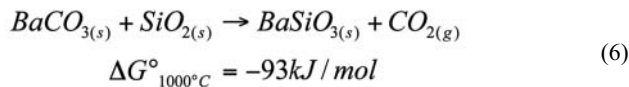
These reactions consume free silica that would otherwise be available for reaction with molten aluminum and result in refractory corrosion. Thus, one aspect of the anti-wetting mechanism provided by BaO addition may be the reduction in free silica available for corrosion.

Albers and Baldo investigated Ba-celsian as a refractory additive¹¹. They added synthetic, monoclinic celsian to a high alumina (85 wt%) refractory castable and studied penetration resistance using molten aluminum in a static cup test at 1000°C. They found that the addition of 3 wt% monoclinic Ba-celsian caused a 50% decrease in the corroded area when compared to compositions without celsian. The polymorphism of Ba-celsian is of interest because Albers and Baldo used monoclinic celsian,

whereas the addition of BaSO₄ leads to the formation of hexagonal celsian within a refractory. Ba-celsian exists in three polymorphs; monoclinic, hexagonal, and orthorhombic¹². The monoclinic phase occurs naturally as a mineral, whereas the hexagonal and orthorhombic phases are synthetic. In the Ba-Al-Si oxide system, the hexagonal celsian phase forms first and can exist as a metastable phase from room temperature to 1590°C. However, the transformation from hexagonal to monoclinic occurs at a very sluggish rate at temperatures above 1200°C^{6, 12, 13}. Schmutzler studied this transformation and found that complete conversion from hexagonal phase to monoclinic phase occurred after annealing at 1200°C for 54 hrs followed by further annealing at 1260°C for 48 hrs¹². This transformation is associated with a volume change of 3-4% and may generate micro-cracks within the refractory¹⁴. On thermal cycling, these cracks can make the matrix more susceptible to aluminum attack. Based on furnace operating temperatures and the transformation temperatures of Ba-celsian, one may conclude that BaSO₄ and BaCO₃ anti-wetting additives form hexagonal Ba-celsian above their decomposition temperature (1150°C) in the refractory during service. Since the hexagonal structure is susceptible to phase transformation at elevated temperatures, monoclinic celsian is the desired stable phase¹²⁻¹⁴.

A review of the open literature revealed that strontium aluminosilicate (Sr-celsian) has many similar properties to those of Ba-celsian^{12, 13, 15}. The synthesis of monoclinic Ba-celsian is a sluggish process^{6, 12}. However, Sr-celsian transforms rapidly at temperatures ranging from 900 to 1200°C¹⁶⁻¹⁸. Such temperatures can be achieved in existing practices. The Sr-celsian transformation will be complete within the heating schedule of the refractory lining. A Sr-celsian matrix within the refractory may improve its stability without the additional heat treatment required by Ba-celsian to stabilize it into its monoclinic form. Since the properties and synthesis routes of Ba-celsian and Sr-celsian are nearly identical, a substitution would not likely affect the thermal-mechanical properties of the refractory linings.

It has been suggested that celsian may decrease wetting of the refractory by molten aluminum or its formation may block the pore channels within the refractory¹⁰. This would lead to densification of the refractory. As described by reactions (2) – (5), the synthesis route of celsian has various silicate phases that may form as intermediate compounds that eventually lead to celsian formation. The presence of a Ba-rich glassy phase as a result of 5 wt% BaO addition to aluminosilicate refractories was reported by Oliveira²³. Oliveira studied the influence of BaO additives on the reaction of aluminosilicate ceramics with molten Al alloys. The addition of small amounts of BaO to the refractory led to a higher densification. It was suggested that a Ba-rich glassy phase was more effective in eliminating porosity than a mullite-based phase^{7, 23}. Allahverdi reported similar observations upon addition of 3.5 wt% BaSO₄ to an aluminosilicate refractory⁷. He attributed densification to a Ba-rich glassy phase, which is likely to be rich in silica. Silica additions to the refractory are made in the form of silica fume, which comprises the matrix of the refractory mix. Since the additives are also in the form of micron size particles, they are incorporated into the matrix. Such conditions within the refractory create a high probability that a barium silicate glassy phase will form by the reaction:



The BaO–Al₂O₃–SiO₂ phase diagram shows that the addition of small quantities of BaO to an aluminosilicate refractory resulted in a composition that lies in the mullite phase field as seen in **Fig. 1**. With the addition of BaO, mullite remained the first crystal formed upon cooling. High-silica refractory compositions containing alumina and small quantities of barium additives generally fall within the composition triangle

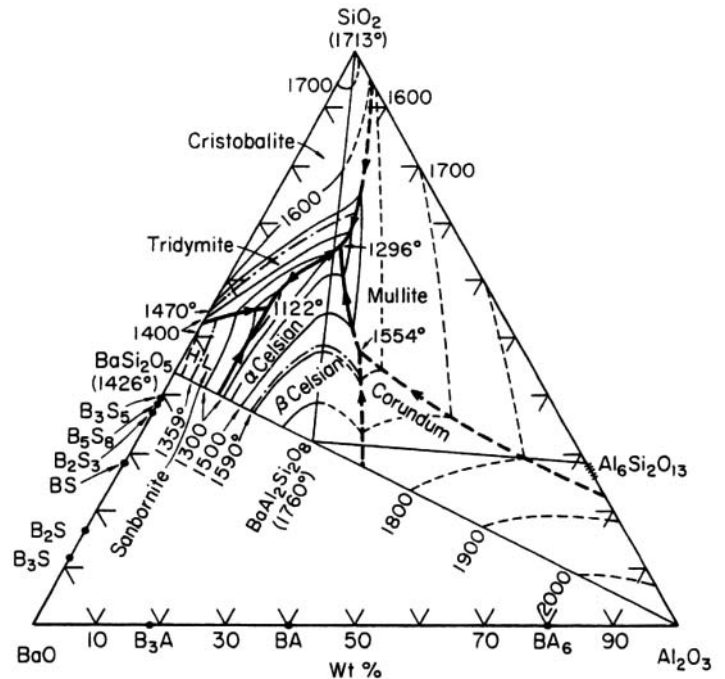


Fig. 1. Phase Diagram of the BaO–Al₂O₃–SiO₂ ternary system²⁷.

BaAl₂Si₂O₈–Al₆Si₂O₁₃–SiO₂ (**Fig. 1**). Thus, mullite crystals will form within a high-silica refractory matrix upon heating and liquid phase sintering, making the refractory susceptible to attack.

The role of Ba-celsian in the non-wetting effect of BaSO₄ additives requires further investigation. It has been suggested that a Ba-rich glassy phase may resist metal attack^{2, 7, 23}. BaO may decrease the wettability of the glassy phase by the molten aluminum²⁵. The celsian may decrease wetting of the refractory by molten aluminum or its formation may block the pore channels within the refractory¹⁰.

Previous works studied the wetting behavior of Ba-celsian and Sr-celsian under identical test conditions¹⁹. Neither material was wet by molten aluminum alloy Al 5083 under a reducing atmosphere (pH₂ = 0.05 atm). **Table 1** summarizes the wetting angles for Ba-celsian and Sr-celsian.

Table 1. Wetting angles of ceramic surfaces¹⁹

| Temperature | Alumina | Ba-celsian | Sr-celsian |
|-------------|---------|------------|------------|
| 800°C | 130±10° | 136±7° | 141±5° |
| 1000°C | 137±6° | 147±7° | 144±4° |

This work investigated the effects of incremental additions of BaCO₃ and SrCO₃ to aluminosilicate refractories. Static cup tests, x-ray diffraction and microscopy techniques were used to investigate the role of these additives in the in-situ formation of celsian within the refractory and its effect on corrosion resistance and porosity.

EXPERIMENTAL PROCEDURE

Sample Preparation

A commercially available aluminosilicate castable was chosen as a base material. Its high silica content would act as starting materials for the formation of desired celsian phases upon heating. The composition of this castable provided by the manufacturer is reported in **Table 2**. The manufacturer indicated that there were no anti-wetting additives in

Table 2. Composition of castable

| Chemical | SiO ₂ | Al ₂ O ₃ | Fe ₂ O ₃ | TiO ₂ | CaO | MgO | Na ₂ O+K ₂ O |
|--------------------------------|-------------------------|--------------------------------|--------------------------------|------------------|-----|-----|------------------------------------|
| wt.% | 45.6 | 42.5 | 0.8 | 1.8 | 2.3 | 0.2 | 0.9 |
| Additives Used | | | | | | | |
| Chemical | Supplier | | Particle Size (µm) | | | | |
| BaCO ₃ | Alfa-Aeser 99.8% Purity | | D ₅₀ = 1.10 | | | | |
| SrCO ₃ | Alfa-Aeser 99% Purity | | D ₅₀ = 1.17 | | | | |
| Al ₂ O ₃ | Almatis A-1000 | | D ₅₀ = 0.3-0.7 | | | | |
| SiO ₂ | Technical Silica Co. | | D ₉₀ < 45 | | | | |

this castable. Since the addition of additives would disturb the optimized particle size distribution of the base mix, 4 wt% silica fume and 4 wt% Al₂O₃ (Almatis A-1000) were added to the base mix described in **Table 2**. This step would provide a better comparison of materials with a modified particle size distribution, such as those containing additives. **Table 2** provides details about various additives used in these experiments. Incremental additions of BaCO₃ and SrCO₃ were made to the base mix as indicated in **Table 3**. The in-situ formation of celsian was investigated in the first stage of experiments. Each composition in **Table 3** was mixed into batches of 1 kg and cast using a vibrating table into cubes (50 mm x 50 mm x 50 mm). The amount of water added was in the range of 5.5 – 6 wt% as prescribed by the refractory manufacturer. The cubes were allowed to cure for 24 hrs and dried at 120°C for another 24 hrs in a drying oven. One cube of each composition was heated to 1200°C and the other was heated to 1300°C in an electrical resistance heated furnace in air atmosphere. The furnace ramp rate was set at 5°C/min and the temperatures were held for 2 hrs. Upon cooling, the cubes were sampled and ground into a powder of fine consistency for powder x-ray diffraction analysis (XRD).

For the static cup test, 9-inch straight bricks (225 x 112 x 63 mm) were cast using vibration with a water content of 5.5 - 6 wt% as recommended by the manufacturer. They were allowed to set for 24 hrs, dried at 120°C for another 24 hrs, and heated to 1200°C for 2 hrs at a heating and cooling rate of 5°C/min. Upon cooling, the bricks were cut in half and a 38 mm diameter core was cut from the center of each half. One half of each brick was then heated to 1300°C at 5°C/min and held for 2 hrs. Thus, there were two cups of each composition, distinguished only by heating temperature. The core cut

Table 3. Phases identified in cup test samples (All samples additionally contain cristobalite and mullite)

| Name | Composition | Temp. | Quartz | Celsian |
|------|---|--------|--------|---------|
| B0 | BM+4%SiO ₂ +4%Al ₂ O ₃ | 1200°C | No | No |
| B0A | BM+4%SiO ₂ +4%Al ₂ O ₃ | 1300°C | No | No |
| B4 | BM + 4 wt% BaCO ₃ | 1200°C | Yes | No |
| B4A | BM + 4 wt% BaCO ₃ | 1300°C | No | No |
| B8 | BM + 8 wt% BaCO ₃ | 1200°C | Yes | Yes |
| B8A | BM + 8 wt% BaCO ₃ | 1300°C | No | Yes |
| B12 | BM + 12 wt% BaCO ₃ | 1200°C | Yes | Yes |
| B12A | BM + 12 wt% BaCO ₃ | 1300°C | Yes | Yes |
| S4 | BM + 4 wt% SrCO ₃ | 1200°C | No | Yes |
| S4A | BM + 4 wt% SrCO ₃ | 1300°C | No | Yes |
| S8 | BM + 8 wt% SrCO ₃ | 1200°C | No | Yes |
| S8A | BM + 8 wt% SrCO ₃ | 1300°C | No | Yes |
| S12 | BM + 12 wt% SrCO ₃ | 1200°C | No | Yes |
| S12A | BM + 12 wt% SrCO ₃ | 1300°C | No | Yes |

from each brick was used to obtain samples for XRD, bulk density and porosity analysis. Bulk density and open porosity were measured as per ASTM C830 standards for measuring porosity of refractories²¹.

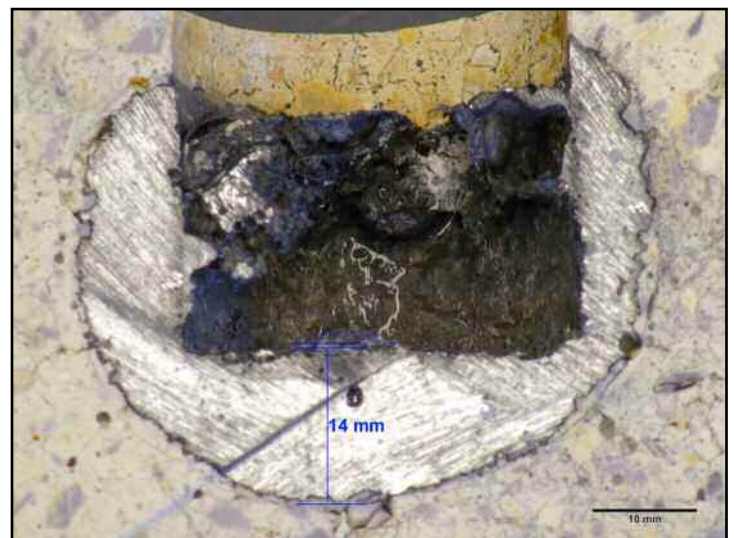
Cup Test Procedure

The static cup tests were performed in a top loaded, electrical resistance heated, box furnace with a hole in the top lid. The test was started by preparing specimens by following the procedure detailed in the previous section. The specimens were placed in the furnace and then heated to 1200°C at a rate of 5°C/min. After holding the temperature at 1200°C for 2 hrs, the temperature ramped down to 1000°C at a rate of 3°C/min. Once this temperature was reached, a water drip system consisting of a steel tube with hose connections was set up at the hole in the lid of the test furnace¹⁹. The water flow rate was maintained at approximately 10 ml/min. The water dripped into the hot furnace and created a H₂/H₂O system at 1000°C. After exposure to this steam atmosphere for 24 hrs, the furnace lid was opened and aluminum alloy pieces placed into the cup test specimens. The aluminum alloy (AL 5083) piece was a 25 mm diameter cylinder of 38 mm height that weighed approximately 70 grams. Once the pieces were placed, the furnace lid was closed and the water drip tube was continued. The steam atmosphere and furnace temperature was maintained for 240 hrs (10 days) and then cooled at a rate of 5°C/min. Cooled samples were sectioned using a masonry saw and the penetration reaction was studied. Appropriate sections of the penetrated area were chosen and mounted in epoxy resin for microscopic analysis. Alloy penetration into the refractory was measured in both sidewalls and the bottom. Since the penetration occurred through the refractory matrix, the reaction did not progress uniformly. The reported value of penetration was the maximum measured penetration occurring in the sample.

Results and Discussion

Powder XRD analysis was performed on the refractory cubes. The base mix (sample B0) consisted of mullite and silica. The XRD analysis revealed that 4 wt% BaCO₃ was not sufficient to form Ba-celsian upon heating to 1200° or 1300°C. All other samples showed celsian peaks along with mullite and cristobalite.

Materials showed significant penetration by molten aluminum alloy. Sample B0 showed the highest penetration. As seen in **Fig. 2**, the maximum penetration was 14 mm. This was the refractory base mix with additional alumina and silica as described in **Table 3**. The heating temperature for this mix was specified at 1200°C. Penetration was nearly identical for samples B4 (10 mm) and B12 (9 mm), while sample B8 (12 mm) showed higher penetration.

**Fig. 2.** Penetration in Sample B0 after static cup test.

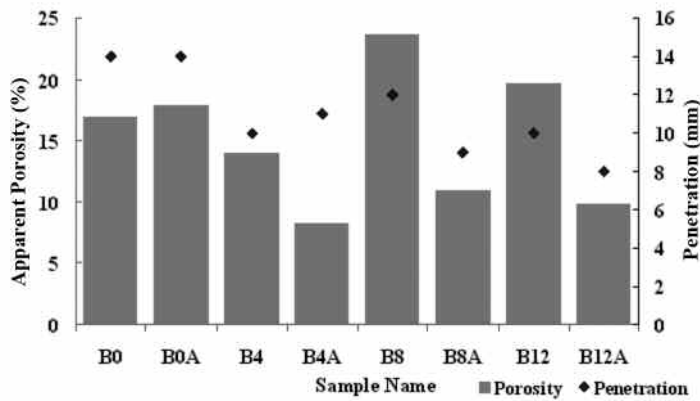
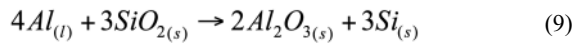
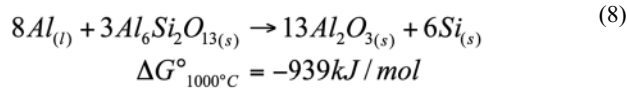


Fig. 3. Penetration and apparent porosity of refractory samples.

Increasing the heating temperature from 1200°C to 1300°C increased the penetration in sample B4A to 11 mm, while it decreased the penetration in samples B8A and B12A by approximately 25%. Overall, the addition of BaCO₃ improved the penetration resistance of all samples compared to the base mix samples. Apparent porosities were measured for all samples and reported in Fig. 3. For each increment of additive, increasing the heating temperature from 1200°C to 1300°C led to a considerable decrease in apparent porosity. The mixes containing BaCO₃ showed an average reduction in porosity of 42%.

Mullite XRD peak intensities reported in Fig. 4 were normalized based on the XRD analysis of sample B0A, which showed the maximum peak intensity for mullite. By increasing the heating temperature, the amount of mullite within the refractory matrix was increased. Mullite is known to be susceptible to attack by molten aluminum².



The presence of high amounts of mullite and free silica in the samples B0 and B0A led to higher penetration by reactions 8 and 9. Sample B0 was analyzed using SEM and EDS techniques. Fig. 5 shows the SEM and EDS maps

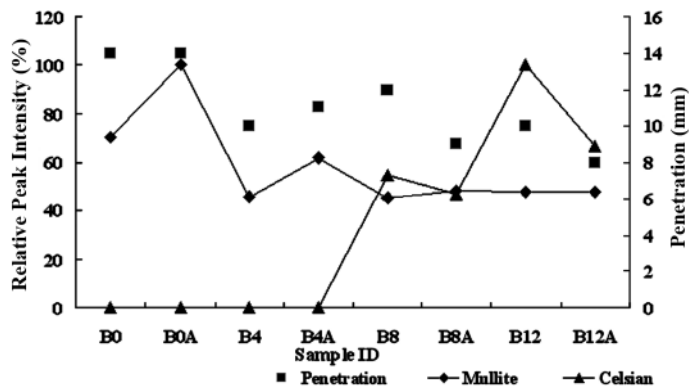


Fig. 4. Relative Peak Intensities from XRD analysis for samples containing BaCO₃.

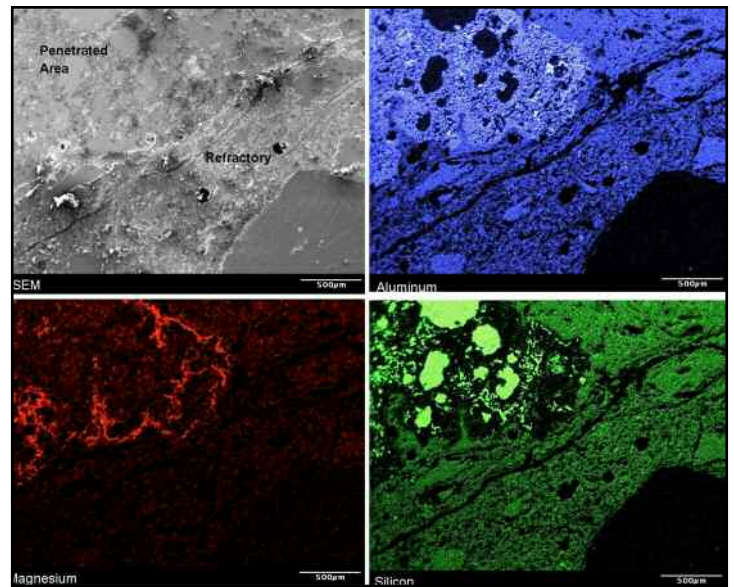


Fig. 5. SEM and EDS analysis of sample B0 after cup testing.

of the penetration interface in sample B0. As expected, the penetrated area was enriched in aluminum. The EDS also detected magnesium in the penetrated area, which came from the alloy (AL 5083). Magnesium is a useful tracing element to determine the extent of penetration using SEM analysis. The silica in the penetrated area is reduced to silicon, which coalesces into spherical drops of metallic silicon in the penetrated area. Such silicon droplets are typically seen in the penetrated area for high-silica refractory cup test specimens.

Effect of BaCO₃ addition

The BaO–Al₂O₃–SiO₂ ternary phase diagram shown in Fig. 1 can represent high-silica refractory compositions containing alumina and barium carbonate additives. Incremental additions of BaCO₃ made per Table 3 resulted in composition that fell within the composition triangle BaAl₂Si₂O₈–Al₆Si₂O₁₃–SiO₂ (Fig. 6). The ternary eutectic for this system is at 1296°C. Upon heating to 1300°C, the refractory matrix sintered by forming a eutectic liquid. The amount of liquid formed depended on the amount of BaO in the starting composition. The starting compositions were within the mullite phase field. Thus, mullite crystals formed within a high silica refractory matrix upon heating and liquid phase sintering, making the refractory susceptible to attack. An analysis at 1300°C for the refractory compositions indicated in Fig. 8 is presented in Table 4.

For a 4 wt% addition of BaCO₃, the amount of eutectic liquid formed at 1300°C was 23%. The eutectic liquid caused a 41% reduction in apparent porosity as reported in Fig. 2. For an 8 wt% addition of BaCO₃, the amount of eutectic liquid formed at 1300°C was 55% leading to a 53% reduction in apparent porosity. For a 12 wt% addition of BaCO₃, the amount of eutectic liquid formed at 1300°C was 43% leading to a 50% reduction in apparent porosity. Thus, an increase in the amount of eutectic liquid led to a lower apparent porosity of the refractory and subsequently an improvement in corrosion resistance. The eutectic liquid contained 46 wt% celsian. The presence of Ba-celsian within the eutectic phase may have provided a more corrosion resistant matrix than a mullite-based refractory such as sample B0A. The analysis at 1300°C also showed that celsian crystals would not form with a 4 wt% addition of BaCO₃. In that case, 83% of the crystals formed were mullite and the remainder was silica. Thus, a 4 wt% addition in fact led to an increase in the mullite content of the refractory. Mullite is susceptible to reaction with molten aluminum and its presence is detrimental to the corrosion resistance of the refractory under these conditions. Samples B4 and B4A, both containing 4 wt% BaCO₃, showed mullite peaks in the XRD analysis.

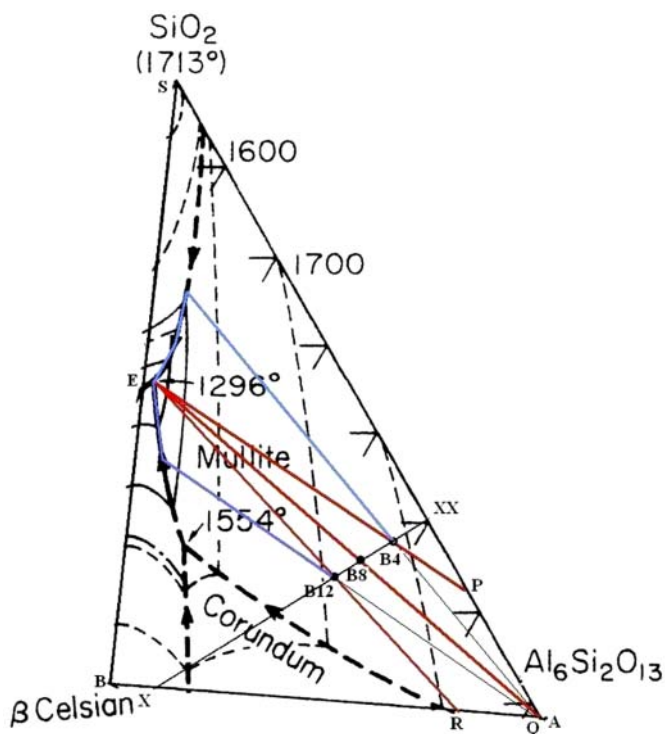


Fig. 6. Composition triangle $\text{BaAl}_2\text{Si}_2\text{O}_8\text{-Al}_6\text{Si}_2\text{O}_{13}\text{-SiO}_2$.

Table 4. Compositional analyses at 1300°C (all values in wt%)

| BaO Content | Solid | | | Liquid |
|-------------|-------------|-------------|------------|--------|
| 4% | 77% | | | 23% |
| | 83% Mullite | 0% Celsian | 17% Silica | * |
| 8% | 45% | | | 55% |
| | 99% Mullite | 1% Celsian | 0% Silica | * |
| 12% | 57% | | | 43% |
| | 87% Mullite | 13% Celsian | 0% Silica | * |

*Eutectic liquid composition (15% Al_2O_3 , 20% BaO, 65% SiO_2)

The peak intensity increased by 50% when heating temperature increased from 1200°C to 1300°C. The increased amount of mullite caused higher corrosion in sample B4A than sample B4.

Analysis of the samples with 8 wt% BaCO_3 suggested that celsian crystals formed at 1300°C. The composition of the crystals was 98.8% mullite and 1.2% celsian. The overall amount of crystals present reduced with an increase in BaCO_3 content from 4 wt% to 8 wt%. The overall amount of mullite crystals was reduced and free silica was consumed in the formation of celsian crystals. The presence of celsian crystals and decrease in the mullite content may have led to an improved corrosion resistance in samples B8 and B8A. The analysis also suggested that the amount of eutectic liquid increased. Along with a greater reduction in apparent porosity than in samples B4A, the celsian-rich eutectic melt phase may have contributed to the improved corrosion resistance. XRD analysis of samples B8 and B8A confirmed the presence of celsian crystals in the refractory matrix. As per the analysis, the celsian content of the formed crystals increased to 7.2% with the addition of 12 wt% BaCO_3 . The amount of eutectic liquid formed was lower than that formed with the 8 wt% addition. Once again, the celsian-rich eutectic liquid caused a reduction in apparent porosity and may have contributed to an improvement in the corrosion resistance along with the celsian crystals present in the matrix.

The XRD and phase equilibrium analysis can also be supported by constructing a vertical section along the line X-XX in Fig. 6. The line X-XX contains the refractory compositions of B4, B8 and B12. The constructed vertical section (Fig. 7) provides a visual reference to the phases formed upon heating the refractory compositions to 1200 and 1300°C. When the refractory composition B4 is heated to 1300°C, sample B4A, it enters a three phase region (mullite + cristobalite + liquid) in Fig. 7. This coincides with XRD analysis presented in Fig. 4. Increasing the BaO content of the refractory and heating to 1300°C shifts the refractory composition into the three phase region (mullite + celsian + liquid). XRD analysis of samples B8A and B12A confirmed the presence of mullite and celsian (Fig. 4). The vertical section supports XRD and phase analysis by indicating that 4 wt% BaO is not sufficient to cause the crystallization of celsian in an aluminosilicate refractory. Based on the vertical section, the BaO content would have to be at least 7 wt% in order to have celsian crystals present within the refractory matrix. Based on literature and results of the present work, the reduction in mullite content can be attributed to the celsian crystallization process. Formation of the celsian crystals also reduced the amount of alumina and silica available for mullite formation and reduced the amount of free silica available for reaction with molten aluminum.

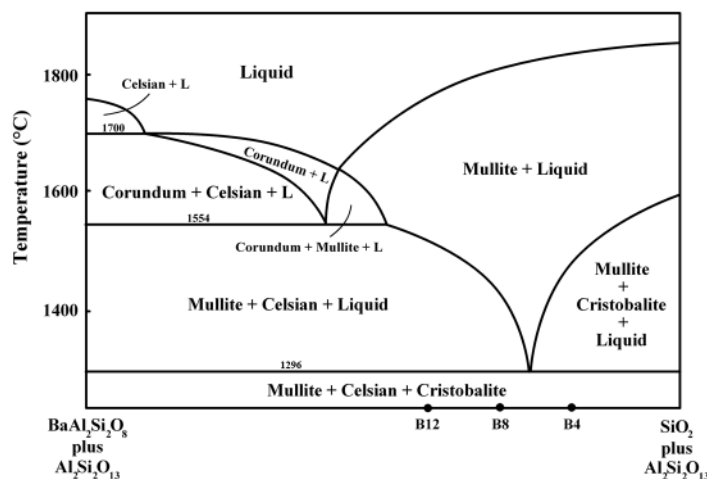


Fig. 7. Vertical section across composition triangle $\text{BaAl}_2\text{Si}_2\text{O}_8\text{-Al}_6\text{Si}_2\text{O}_{13}\text{-SiO}_2$ along line X-XX in Fig. 6.

The densification of the refractory matrices because of the addition of BaCO_3 and heating to 1300°C was clearly visible by comparing scanning electron microscopy (SEM) images of samples B0A and B12A seen in Fig. 8. The refractory matrix for sample B0A was an intricate network of micron-sized pores. Addition of BaCO_3 blocked this network with the eutectic liquid formed at 1300°C in sample B12A. Energy dispersive spectroscopy (EDS) was conducted on the matrix of sample B12A. EDS analysis revealed that the dense matrix consisted of barium, aluminum and silicon. This phase may have led to an improvement in the corrosion resistance of the refractory, as per suggestions in literature that barium-rich glassy phases can resist aluminum attack⁷. EDS elemental mapping of the sample confirmed that barium was present only in the refractory matrix, as intended. Fig. 9 shows the elemental map for barium in sample B12A. Compared to the SEM image of the penetration interface, the barium elemental map showed vacant, dark spots wherever aggregate grains or open pores were present.

Effect of SrCO_3 addition

The effect of the addition of 4, 8 and 12 wt% SrCO_3 to the base mix was studied at heating temperatures of 1200°C and 1300°C by cup testing at 1000°C. Samples S4, S8, and S12 had nearly identical penetration, whereas a decreasing penetration trend was observed with samples S4A, S8A, and S12A.

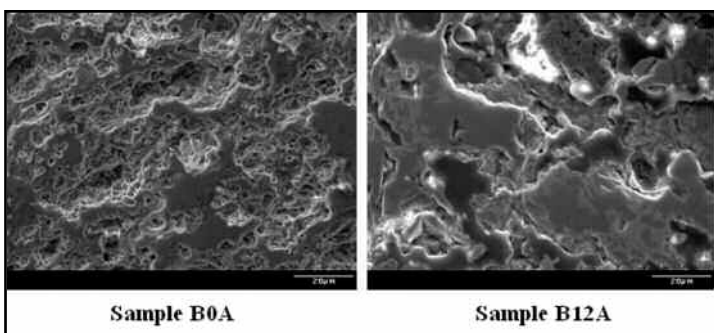


Fig. 8. Effect of eutectic liquid on porosity of refractory.

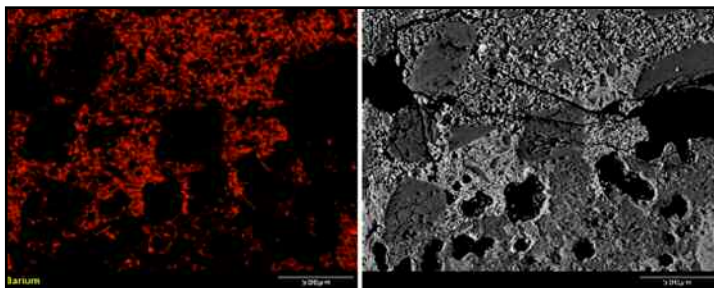


Fig. 9. EDS elemental map of barium in sample B12A.

Increasing the amount of additive had no visible effect on corrosion resistance upon heating to 1200°C. Samples S4, S8, and S12 showed identical penetration (10 mm) in the cup test as reported in Fig. 10. The penetration data suggested that the addition of SrCO₃ to a high-silica aluminosilicate refractory reduced penetration by approximately 35%. Comparison of apparent porosities reported in Figs. 3 and 10 revealed that increasing the heating temperature from 1200°C to 1300°C did not promote densification of the refractory as much as in the refractories containing BaCO₃. The mixes containing BaCO₃ showed an average reduction in porosity of 42%. The average reduction in porosity for mixes containing SrCO₃ was only 20%. For refractories heated to 1200°C, the penetration was proportional to the apparent porosity of the samples.

A detailed phase diagram with liquidus projections for the SrO–Al₂O₃–SiO₂ system was not available and published literature addressed only the alkemade lines with binary and ternary compounds^{17, 18}. The only available phase diagram is shown in Fig. 11. Similar to the BaO–Al₂O₃–SiO₂ system, the system in Fig. 11 also has a composition

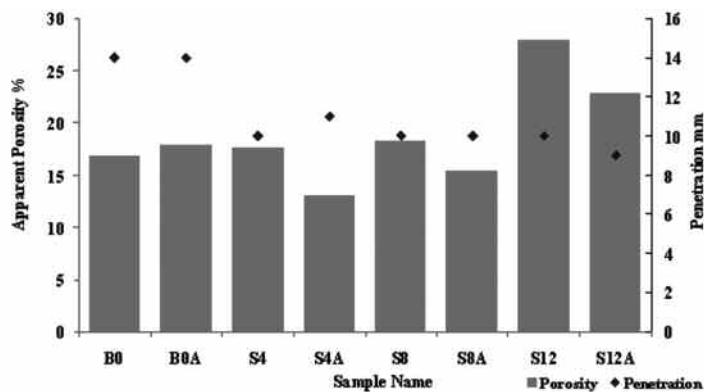


Fig. 10. Penetration and porosity in SrCO₃ samples.

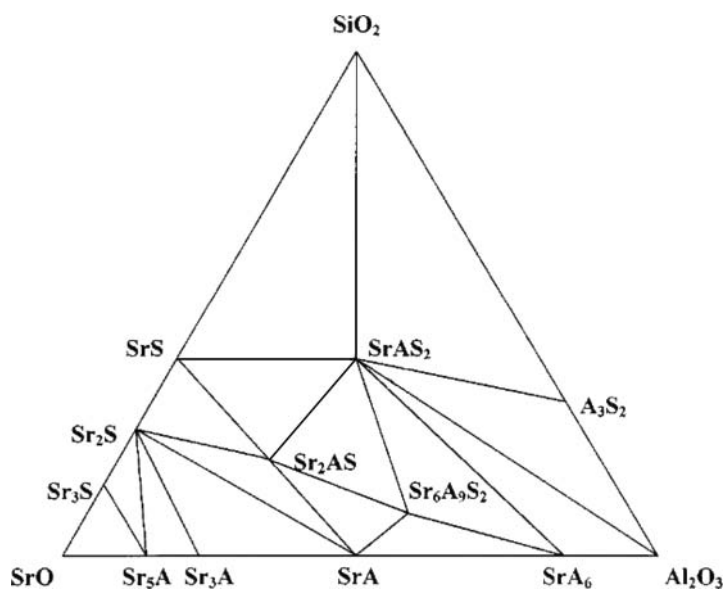


Fig. 11. Phase stability diagram of SrO–Al₂O₃–SiO₂¹⁷.

triangle of mullite–celsian–silica. The incremental additions of SrCO₃ made according to Table 2 would result in compositions that were within this composition triangle. Hence, the addition of SrCO₃ to the refractory mix would lead to the formation of mullite along with Sr-celsian. Since the ternary eutectic points and phase boundaries are not available for this system, a detailed analysis could not be performed to estimate the amount of crystals formed, or the role of liquid phase sintering in reducing apparent porosity. However, some analogies may be drawn by comparing the XRD data with the analysis of the samples containing BaCO₃.

XRD analysis confirmed the presence of monoclinic Sr-celsian in all samples. The addition of 4 wt% SrCO₃ was successful in creating celsian crystals within the refractory as shown by the XRD data. The Sr-celsian peak intensity increased with increased amounts of SrCO₃ additive. Correspondingly, the relative peak intensities for mullite decreased. The formation of celsian crystals decreased the mullite content of the refractory matrix by consuming alumina and silica. From the apparent porosity measurements, it appeared that the ternary eutectic point for the mullite–celsian–silica system in Fig. 11 is above 1300°C. This would explain why the increase in heating temperature did not cause a significant reduction in apparent porosity.

Another explanation of the poor densification may be provided by considering the premature crystallization of Sr-celsian as shown in Fig. 12. Literature on the formation of Sr-celsian reported that crystallization temperature and sintering temperature for SrO–Al₂O₃–SiO₂ glassy phases were not always identical. Sung found that the presence of nucleating agents such as TiO₂ could reduce the crystallization temperature of Sr-celsian and cause premature crystallization at 950–1050°C, while liquid phase sintering would occur at 1550°C²⁶. A similar nucleating effect of TiO₂ on the devitrification of cordierite was observed by Weaver et al.²⁷. Such crystallization occurred directly into monoclinic Sr-celsian rather than following the conventional sequence of hexagonal celsian formation and its subsequent transformation into the desired monoclinic phase as described by Bansal¹². The nucleating effect of TiO₂ may have caused premature crystallization of monoclinic Sr-celsian within the refractory. Crystallization of Sr-celsian at lower temperatures altered the chemistry of the remaining liquid phase, reducing the amount of free silica present and the amount of mullite formed at

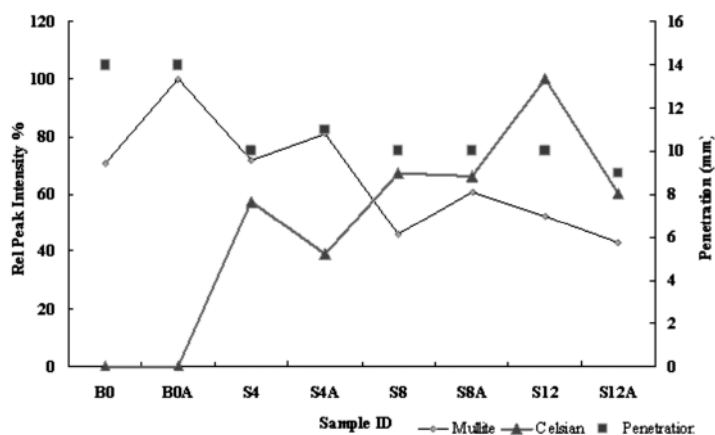


Fig. 12. Relative Peak Intensities from XRD analysis for samples containing SrCO₃.

higher temperatures. Monoclinic Sr-celsian was the desired phase to be formed by the addition of SrCO₃ in the refractory. However, the premature crystallization did not cause a reduction in apparent porosity. EDS analysis of the refractory matrix in sample S12 revealed that TiO₂ was indeed present in the refractory matrix. Thus, the SrCO₃ additives were not capable of creating a significant reduction in apparent porosity that would lead to an improvement in the corrosion resistance of the refractory.

Conclusions

The effect of BaCO₃ and SrCO₃ on the corrosion resistance of a high-silica aluminosilicate castable refractory to molten aluminum alloy was evaluated with static cup testing. These additives were not able to improve the penetration resistance when the refractory was heated to 1200°C. Based on the phase diagram, XRD analysis and phase equilibrium analysis of the refractory compositions, it was seen that the additions of BaCO₃ formed Ba-celsian, and led to the formation of mullite. Although the formation of Ba-celsian consumed some free silica, mullite and cristobalite peaks were identified in the XRD analysis. Thus, at 1200°C, the additives inadvertently exacerbated the corrosion resistance of the refractory by promoting the formation of mullite. Upon heating to 1300°C, the refractories containing BaCO₃ showed significant reductions in apparent porosity. Based on the phase equilibrium analysis, it was suggested that the eutectic liquid formed at 1296°C caused this reduction in porosity via liquid phase sintering. The presence of a celsian-rich eutectic melt phase within the refractory matrix along with Ba-celsian crystals improved corrosion resistance when heated to 1300°C. It was seen that addition of 12 wt% BaCO₃ and heating to 1300°C provided a better corrosion resistance than the base mix heated to 1300°C.

Addition of SrCO₃ to the refractory mix also promoted mullite formation. Hence, the samples heated to 1200°C were penetrated more than the base mix composition. The analysis of the samples containing SrCO₃ was limited by the availability of a complete phase diagram. Upon heating to 1300°C, the reduction in apparent porosity was not as significant as in the samples containing BaCO₃. This suggested that significant liquid phase sintering did not occur in the samples heated to 1300°C. The presence of TiO₂ caused premature crystallization of the Sr-celsian. This prevented the formation of a Sr-celsian-rich, eutectic melt phase that could reduce the apparent porosity and provide the pore-blocking effect as was originally intended. Previous work on the wetting behavior of celsian crystals has shown that both, Ba-celsian and Sr-celsian are not wet by molten aluminum at 1000°C. It was intended that the presence of these crystals within the refractory matrix would provide a non-wetting effect and prevent corrosion. It was also expected that the celsian-rich glassy phases would

cause a pore-blocking effect and prevent metal penetration into the refractory matrix. Such a densification was not observed in the samples containing Sr-celsian, but was successfully created with Ba-celsian. This suggests that the reduction in porosity by a non-wetting medium can improve the corrosion resistance of the refractory. Although the current work successfully reduced the apparent porosity of tested samples, the role of pore size distribution has not been considered. Future work should address the impact of the in-situ formation of Ba-celsian on the pore size distribution.

References

- ¹C. Allaire and S. Afshar, "Furnaces: Improving Low Cement Castables by Non-Wetting Additives", *JOM*, **53** [8] 24-27 (2001).
- ²S. Afshar and C. Allaire, "The Corrosion of Refractories by Molten Aluminum", *JOM*, **48** [55] 23-27 (1996).
- ³R. Talley, R. Henriksen and W. Bakker, "Refractories for Aluminum Melting Furnaces", U.S. Patent 4522926 (11 June 1985).
- ⁴J. Teiken and L. Krietz, "Additive Effects on the Physical Properties of Castable Systems for Aluminum Contact Applications", 9th Symposium on refractories for the Aluminum Industry, TMS, Warrendale, PA, 2000.
- ⁵S. Ketchion, J. Coppack and L. Williams, "High Temperature Corrosion Resistance of Aluminum Contact Refractories", 384-385 *Proceedings of UNITECR*, Berlin, Germany, 6-9 September, (1999).
- ⁶H. Schmutzler and K. Sandhage, "Transformation of Ba-Al-Si Precursors to Celsian at High-Temperature Oxidation and Annealing", *Metall. Mater. Trans B*, **26** [1] 135-148 (1995).
- ⁷M. Allahevrdi, S. Afshar and C. Allaire, "Additives And The Corrosion Resistance Of Aluminosilicate Refractories In Molten Al-5Mg", *JOM*, **50** [2] 30-34 (1998).
- ⁸K. Brondyke, "Effect of Molten Aluminum on Alumina-Silica Refractories", *J. Am. Ceram. Soc.*, **36** [5] 171-174 (1953).
- ⁹S. Gupta, P. Koshy and V. Sahajwalla, "Influence of Non-wetting Agents on the Modification of Dynamic Wetting of High Alumina Monolithic Refractories by Aluminum Alloy", 630-633, *Proceedings of UNITECR*, Orlando, FL, USA, 8-11 November, (2005).
- ¹⁰J. Aguilar-Santillan and R. Bradt, "Wetting of Al₂O₃ by Molten Aluminum: The Effects of BaSO₄ Additions", *Journal of Nanomaterials*, 35-63, (2008).
- ¹¹A. Albers and J. Baldo, "Improving the Corrosion Resistance of Low Cement Aluminum Silicate Refractories Castable in Contact with Molten Alloyed Aluminum", *Light Metals Age*, 34-41 (2001).
- ¹²N. Bansal, "Solid State Synthesis and Properties of Monoclinic Celsian", *J. Mater. Sci.*, **33** [19] 4711-4715 (1998).
- ¹³Y. Kobayashi, "Transformation Kinetics From Hexacelsian To Celsian For Powders Having Uniform Particle Size", *Ceram. Int.*, **27** [2] 179-184 (2001).
- ¹⁴N. Bansal and M. Hyatt, "Crystallization Kinetics of BaO-Al₂O₃-SiO₂ Glasses", *J. Mater. Res.*, **4** [5] 1257-1265 (1989).
- ¹⁵Y. Fu, C. Chang, C. Lin and T. Chin, "Solid State Synthesis of Ceramics in the BaO-SrO-Al₂O₃-SiO₂ System", *Ceram. Int.*, **30** [1] 41-45 (2004).
- ¹⁶Y. Kobayashi and M. Inagaki, "Preparation of Reactive Sr-celsian Powders by Solid-state Reaction and their Sintering", *J. Eur. Ceram. Soc.*, **24** [2] 399-404 (2004).
- ¹⁷Y. Sung and S. Kim, "Sintering and Crystallization of Off-Stoichiometric SrO•Al₂O₃•2SiO₂ Glasses", *J. Mater. Sci.*, **35** [17] 4293-4299 (2000).
- ¹⁸Y. Sung, "Crystallization of Celsian Glasses of (SrO•Al₂O₃•2SiO₂)-(Al₂O₃) Pseudo-Binary Compositions", *J. Mater. Sci. Lett.*, **20** [9] 839-840 (2001).
- ¹⁹D. Shukla, W. Headrick, and J. Smith, "Testing of Advanced Refractory Materials", Proceedings of Materials Science & Technology Conference, Cincinnati, OH, USA, 15-19 October (2006).
- ²⁰American Society for Testing of Materials, "Annual Book of ASTM Standards", (2001).
- ²¹E. Levin, C. Robbins and H. McMurdie, "Phase Diagrams for Ceramists: Supplement", The American Ceramics Society, (1974).
- ²²M. Oliveira, S. Agathopoulos and J. Ferreira, "The Influence of BaO Additives on the Reaction of Al₂O₃SiO₂ Ceramics with Molten Al and Al-Si Alloys", *Acta Mater.*, **50** [6] 1441-1451 (2002).
- ²³E. Levin, C. Robbins and H. McMurdie, "Phase Diagrams for Ceramists: Volume 1", The American Ceramics Society, (1964).
- ²⁴O. Siljan, G. Rian, D. Pettersen and A. Solheim, "Refractories for Molten Aluminum contact Part 1: Thermodynamics and Kinetics", *RAN*, **7** [6] 17-25 (2002).
- ²⁵D. Weaver, D. Van Aken and J. Smith, "The Role of TiO₂ and Composition in the Devitrification of Near Stoichiometric Cordierite", *JOM*, **39** [1] 51-59 (2004).